Role of resonances in the electron-impact excitation functions of the $C\ ^3\Pi_u$ and $E\ ^3\Sigma_g^+$ states of N_2†

D. E. Golden, D. J. Burns, and V. C. Sutcliffe, Jr.
Behlen Laboratory of Physics, University of Nebraska, Lincoln, Nebraska 68508
(Received 20 May 1974)

Resonances in e^--N_2 scattering have been studied from about 11 to 16 eV by simultaneous measurement of the transmitted electron spectrum, and both the prompt and delayed emission functions for the $C\ ^3\Pi_u \rightarrow B\ ^3\Pi_g(0,0)$ transition. In this energy domain 28 structures have been observed, 25 of which have been observed in both the electron transmission spectrum and the total optical excitation function. The delayed emission in this energy range is attributed to the decay of the various states of N_2^- to the $E\ ^3\Sigma_g^+$ state of N_2 which is collisionally de-excited to the $C\ ^3\Pi_u$ state of N_2. Negative-ion resonances which decay to both the $E\ ^3\Sigma_g^+$ and $C\ ^3\Pi_u$ contribute strongly to the 3371 emission in this energy domain.

INTRODUCTION

The energy region between about 11.5 and 15 eV in e-N_2 scattering has much structure attributable to the temporary formation of various N_2^- states which have been observed using a variety of measurement techniques.[1]

The Feshbach resonance at 11.48 eV, first observed by Heideman, Kuyatt, and Chamberlain in a transmission experiment,[2] has been classified as $^2\Sigma_g^+$ by Comer and Read,[3] and is likely to be the first member of a vibrational series of Feshbach resonances associated with the closed $E\ ^3\Sigma_g^+$ channel and consisting of two $3s\ \sigma_g$ electrons temporarily bound to an $N_2^+\ ^2\Sigma_g^+$ core.[1] The first of this "b" series of resonances has also been observed as a sharp peak in the optical excitation of the $C\ ^3\Pi_u$ state of N_2 by Kisker.[4] Furthermore, Finn *et al.* have observed structure near the thresholds of the emission functions of the second positive system of N_2.[5]

A peak just above the $E\ ^3\Sigma_g^+$ threshold at 11.92 eV in the electron transmission spectrum has been identified as a p-wave shape resonance associated with the $E\ ^3\Sigma_g^+$ threshold at 11.87 eV.[6] This core-excited shape resonance has also been identified as the first member of a series of resonances associated with the thresholds of the vibrational levels of $E\ ^3\Sigma_g^+$ and designated $^2\Sigma_u^+$.[7] Structure in the excitation of the $E\ ^3\Sigma_g^+$ has also been observed in the cross section for the production of metastables by electron impact,[8] by using a surface ionization detector to detect the metastables. By studying the optical emission from an excited molecular beam Freund[9] found the emission function for the $C\ ^3\Pi_u \rightarrow B\ ^3\Pi_g(0,0)$ band to have a resonant excitation peak which he concluded was due to cascade from the E to the C state.

Kurzweg, Egbert, and Burns,[10] by using a delayed coincidence technique between exciting electrons and the subsequent photons, were able to separate the emission of the $C\ ^3\Pi_u \rightarrow B\ ^3\Pi_g(0,0)$ at 3371 Å into a component due to direct excitation of the $C\ ^3\Pi_u$ and a delayed component due to cascade from the $E\ ^3\Sigma_g^+$. The delayed emission function showed a sharp peak at 12 eV with subsidiary features at 12.7 and 22 eV. They also showed that the lifetime of the prompt radiation due to the natural lifetime of the C state was 37.4 nsec while the lifetime of the delayed radiation had a pressure dependent lifetime of about 10 μsec at a pressure of about 20 mTorr.

Recently, it has been shown by Golden and Ormonde,[11] that at the position of a negative-ion resonance an inverted population may be maintained by electron impact alone under proper conditions. Since the $C \rightarrow B$ emission has been shown to contain significant resonant contributions, in the light of the prediction of Golden and Ormonde,[11] it would seem worthwhile to further investigate the excitation and deexcitation of the $C \rightarrow B$ transition at high electron energy resolution.

This paper reports measurements with high electron-energy resolution of both the prompt and delayed emission functions for the $C\ ^3\Pi_u \rightarrow B\ ^3\Pi_g(0,0)$, 3371-Å transition and the electron transmission spectrum in N_2 for an energy region from about 11 to 16 eV.

APPARATUS AND PROCEDURE

The experimental arrangement which consists of a modulated electron gun, a gas target, and an electron multiplier housed in a vacuum system, together with a monochromator, a photomultiplier, a phase-sensitive detector, timing circuits, and two multichannel analyzers is shown schematically on Fig. 1.

The electron gun used in this work is essentially the same as that described previously,[12] with the

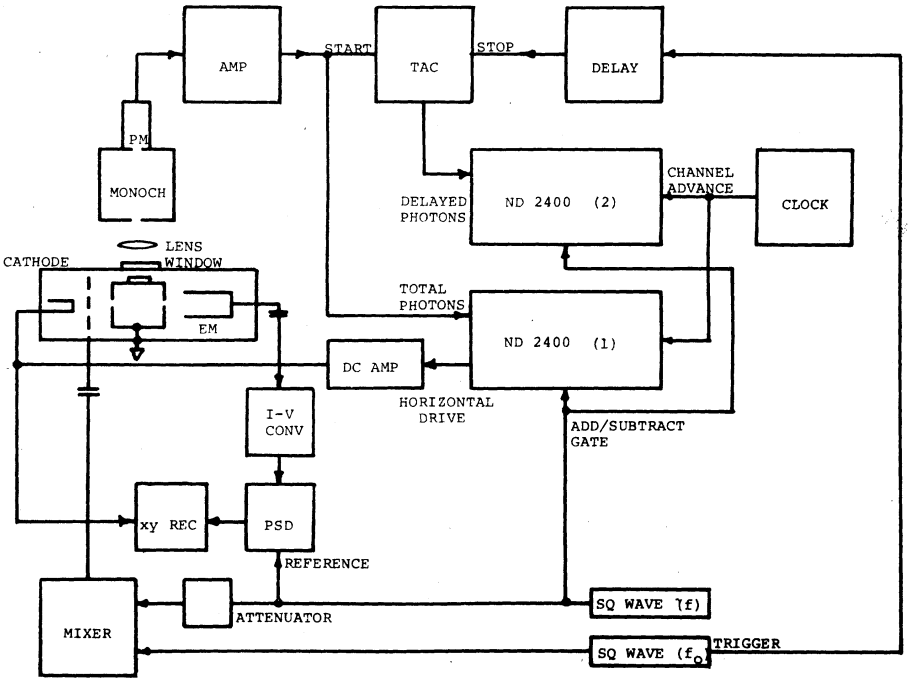

FIG. 1. Experimental arrangement.

following exceptions. The scattering cell has been increased in length to 4.6 cm in order to accommodate a 1.27-cm-diam quartz window perpendicular to the axis of the electron beam. The inside of this window has been covered with a copper mesh of 90% transmission in order to shield the electron beam from it electrostatically. In order to accommodate this longer scattering cell on the existing supports, lens element six[13] has been removed. In the present configuration the electron current used was about 10^{-7} (A/eV) ΔE, where ΔE is the full width at half-maximum (FWHM) defined by the modulation at frequency f and applied to the retarding element shown schematically on Fig. 1. Over the range of energies used in this work the electron beam current was adjusted to be constant to within ±2%. In the present usage, the electron current is pulsed by a square wave of frequency f_0 (~40 kHz) which is amplitude modulated by another square wave of frequency f (~400 Hz) applied to the retarding element of the electron gun. With this applied modulation, the electron gun is either off or on at operation points A or B as shown on Fig. 2. When the electron gun is at operating point A, only electrons in the cathode distribution whose energies are greater than E_A are allowed to reach the interaction region, while when the electron gun is at operating point B, only electrons in the cathode distribution whose energies are greater than E_B are allowed to reach the interaction region. It has been shown that the signal in phase with the modulation at f is proportional to scattering, with an effective energy width $(E_B - E_A)$.[14]

Thus when modulation at frequency f is applied to the retarding element, the transmitted current $I_t(E)$ at energy E, in phase with the modulation at frequency f, is given by[14]

$$I_t(E) = \int_{E+E_A}^{E+E_B} F(E' - E) \exp[-\sigma_t(E')nx]\, dE', \quad (1)$$

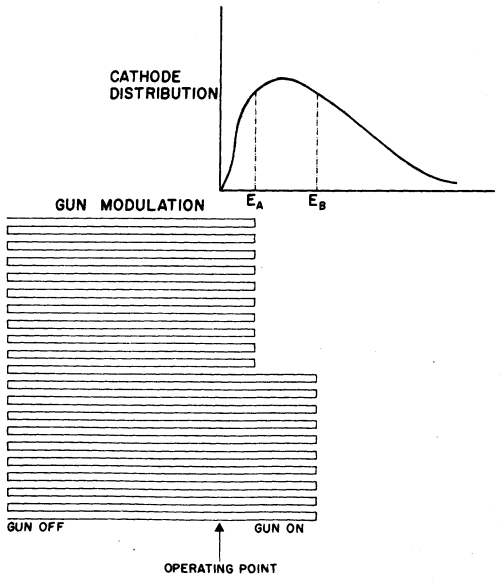

FIG. 2. Modulation wave form as applied to the electron energy distribution leaving the cathode.

where $F(E'-E)$ is the current distribution leaving the cathode, E_A and E_B are the two low-energy cutoffs applied at the retarding element, E is the energy added between the retarding element and the interaction region, $\sigma_t(E)$ is the total scattering cross section at energy E, n is the gas density in the interaction region, and x is the path length of the electron beam through the gas. In a similar manner, for an excitation cross section $\sigma_i(E)$ which is small, that is for $\sigma_i(E)nx \ll 1$, the number of excitations of state i created per second,

$$\frac{dN_i}{dt}(E),$$

is given by

$$\frac{dN_i}{dt}(E) = \frac{1}{e}\int_{E+E_A}^{E+E_B} F(E'-E)\sigma_i(E')nx\,dE', \qquad (2)$$

where e is the electron charge.

Although most of the results to be presented below were obtained by applying the wave form shown on Fig. 2 to the retarding element, some transmitted-electron spectra were also obtained by applying the modulation at frequency f to the interaction region. In such a case it has been shown that the retarded energy-modulated transmitted electron current, in phase with the applied modulation, is given by[14]

$$I_t(E) = -\int_{E+E_A}^{E+E_B} F(E'-E)\exp[-\sigma_t(E')nx]\,dE' + \Delta E\int_{E+E_B}^{\infty}\frac{dF}{dE'}(E'-E)\exp[-\sigma_t(E')nx]\,dE', \qquad (3)$$

where if $\sigma_t(E)$ is a slowly varying function of energy, $I_t(E)\sim 0$, and if $\sigma_t(E)$ is a rapidly varying function of energy, $I_t(E)$ is composed of two terms. The first term is exactly the same as that given above by Eq. (1), while the second term is slowly varying.[14] Thus, shifting the modulation to the interaction region allows the detection of sharp structure while removing the slowly varying background changes in the transmitted current due to both scattering and electron optics effects.

In order to measure transmitted electron spectra, the electrons passing through the interaction region were detected by an electron multiplier. The output of the multiplier was capacitively applied through a current-to-voltage converter to a phase sensitive detector referenced to f. The transmitted electron signal (phase sensitive detector output) was either plotted as a function of electron energy (voltage between cathode and interaction region) directly on an xy recorder, or was stored in a multichannel scalar by connecting the output of the phase-sensitive detector through a voltage-to-frequency converter to the input of the multiscalar, in which each channel address corresponds to a specific electron energy.

When sweeping the electron energy, the sweep speed used was 300 sec/V and the response time of the phase sensitive detector was 3 sec. When stepping the electron energy, the horizontal drive of one multiscalar was used to vary the electron energy in the interaction region by preset steps of any even multiple of 2 mV/step. For most of the work reported here, the step size used was 16 mV. Thus the reproducibility of features is about ±20 meV. A current integrator was used as a clock by integrating a preset fixed current to obtain a selected charge. When the selected charge was obtained, an output pulse from the integrator was used to develop a channel advance pulse which was applied to all multiscalars used. Thus each channel address in each multiscalar corresponds to a particular electron energy with the dwell time at each electron energy equal to some preselected amount, generally 162 sec.

Photons from 1.27 cm of the electron beam were observed at 90° by a monochromator-photomultiplier. A quartz lens of 75-mm focal length focused an image of the beam along the 2-mm entrance slit of an $f/6.8$ monochromator. The band pass of the monochromator was 40 Å. Photons passing through the monochromator were detected by a cooled RCA 31034A photomultiplier. The output pulses from the photomultiplier were applied through a timing amplifier and discriminator to a multiscalar [ND(1)] which was used to record a signal proportional to the total emission as a function of electron energy. When counting photons, each multiscalar used to store the counts was gated to add in phase with and subtract out of phase with the low-frequency modulation f. The emission function thus determined is that characteristic of an energy distribution of width $E_B - E_A$.

In order to study contributions to the particular emission function due to cascade from longer-lived states, the method of delayed coincidence of Kurzweg, *et al.*[10] was used. In the present arrangement, a pulse from the amplifier discriminator was used to start a time-to-amplitude converter (TAC). A trigger pulse from the pulser at f_0 was applied through an appropriate delay generator (so as to exclude both photons generated during the exciting pulse and prompt photons emitted during the off time of the gun) to the stop gate of the TAC. Thus output pulses from the TAC correspond to photons delayed by any time greater than the prescribed time set by the delay generator. This time delay was adjusted while studying the pulse height distribution of output pulses from the TAC by using a pulse-height analyzer in place

of ND(2). The pulse-height analyzer was also used to study the various lifetimes contributing to the decay of the state being studied by the monochromator. These results were in agreement with those reported previously.[10] After the time delay adjustment, the output of the TAC was applied to the multiscalar ND(2) which was used to store the delayed photon-emission function.

Nitrogen gas (99.9% pure) was allowed to enter the gas cell through a leak valve (not shown on Fig. 1) and effuse out through the 1-mm entrance and exit apertures for the electron beam. The gas pressure was measured by a Schulz-Phelps high-pressure ion gauge,[15] connected to the gas cell. Rough energy scale calibration (~0.15 eV) was accomplished by measuring the voltage between the retarding element and the interaction region with the electron gun tuned to allow maximum electron transmission and steady-state gas flow established at the operating pressure. High-sensitivity energy-scale calibration was accomplished by running a retarded energy-modulated transmitted-electron spectrum of N_2, calling the position of the lowest-energy feature in this energy domain 11.48 eV.[2] Since this modulation procedure eliminates much of the slowly varying contributions to the transmitted electron signal, it allows accurate relative position observations of resonance effects. The electron energy-scale calibration was extended to the photon channels by simultaneous measurement of the transmitted electron spectrum with the total-emission function and/or delayed-emission function.

RESULTS AND DISCUSSION

An example of retarded, energy-modulated[14] data are shown on Fig. 3 for a range of energies from about 11 to 14.5 eV. This is a tracing of the spectrum directly plotted on an x-y recorder as outlined above. Figure 3(b) is a continuation of Fig. 3(a) above 12.9 eV. Since the transmitted electron current is dependent on the total scattering cross section [see Eq. (3)] and the elastic-scattering cross section is large compared to the various inelastic-scattering cross sections in this energy domain,[16] the various structures observed on Fig. 3 are to be interpreted as being mainly due to the decay of the various negative-ion states through the elastic channel. We will discuss the features observed on Fig. 3 when we summarize all of the features below.

The decay of these resonances into the E and C states may be seen by directly studying the light emission. When a particular resonance energy is reached, the optical emission is enhanced.

In Fig. 4 we show a plot of the total emission function [ND(1)] for N_2 $C\,^3\Pi_u - B\,^3\Pi_g(0,0)$ for an energy resolution of about 300 meV (no modulation applied to the multiscalar), a gas pressure of about 20 mTorr, and an electron beam current of about

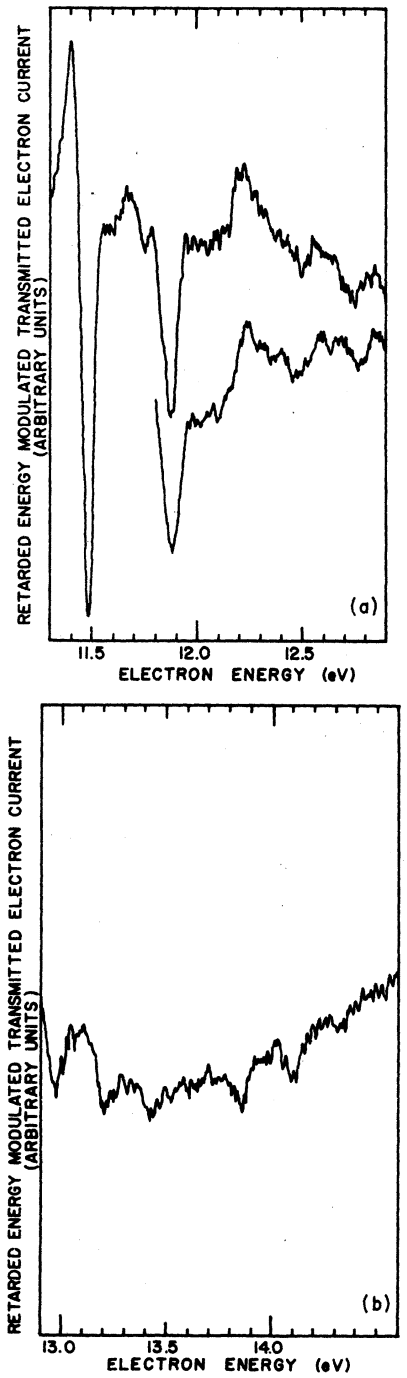

FIG. 3. Retarded energy-modulated transmitted-electron spectrum of N_2 at 50-meV energy resolution for a range of energies from (a) 11.3 to 12.9 eV, (b) 12.9 to 14.6 eV.

3×10^{-8} A. Even at this energy resolution, which is given by the full distribution leaving the cathode, much structure which can be correlated with structure in the transmitted electron spectrum may be seen. A detailed discussion of this structure is postponed until the higher-resolution data is discussed. The threshold energy of this state is at 11.02 eV, and above threshold the emission function rises to a peak at about 14 eV and then falls off rapidly as one goes to higher energies. For comparison the previous total-emission results of Burns, Simpson, and McConkey,[17] and the prompt emission results of Kurzweg *et al.*[10] (normalized to the present results at 14 eV) are also shown. The results of Burns *et al.*,[17] are in agreement with the results of Jobe, Sharpton, and St. John[18] and Aarts and DeHeer,[19] which are not shown. At 16 eV, the emission function has dropped by about a factor of two from its value at 14 eV, which is in good agreement with the results of Kurzweg *et al.*[10] One might expect such a sharply peaked emission function for the C state since we are dealing with a triplet upper state. In the case of electron impact excitation of He, Ormonde and Golden,[20] have suggested that temporary negative-ion formation be considered as a mechanism for triplet excitation. In such a case, triplet excitation arises naturally from the spontaneous decay of the negative ion and one does not need to flip a spin as is necessary for direct triplet excitation. In the present case, either the negative-ion state giving rise to the 14-eV peak in the $C\,^3\Pi_u \rightarrow B\,^3\Pi_g$ transition would have a very short lifetime ($\sim10^{-16}$ sec) corresponding to the width of the peak, or many overlapping longer-lived negative-ion states would contribute to the peak. As will be seen below, the latter appears to be the case. It has been further suggested by Golden and Ormonde[11] that if an excitation cross section by electron impact is resonant, then one would expect the deexcitation cross section by electron impact to be significantly smaller than the excitation cross section at the resonance energy.[21] Furthermore, if the ratio of excitation to deexcitation by electron impact is sufficiently large, a laser can be constructed simply by using an electron beam incident on the target atom or molecule.[11,21] It should be noted that both the Born approximation calculation of Stolarski *et al.*,[22] and the Ochkur-Rudge approximation of Cartwright,[23] neither of which can account for a resonance mechanism, give a much broader peak for the direct excitation of $C\,^3\Pi_u$ than that given by the absolute measurements of the excitation function for $C\,^3\Pi_u \rightarrow B\,^3\Pi_g$ of Burns *et al.*[17] Using the results of Burns *et al.*[17] for the ratio of excitation of the C state at 14 eV to that at 25 eV in the two level calculation of Golden and Ormonde,[11] one gets a value of two for the ratio of the excitation cross section to the deexcitation cross section of the C state at 14 eV.

Figure 5 shows an example of the outputs of (a) the total photon channel [ND(1)] and (b) the delayed photon channel [ND(2)]. Figures 5(a) and 5(b) were run at 100-meV energy resolution simultaneously with a transmitted electron spectrum run on an x-y recorder in order to cross calibrate the electron energy scales from the position of the 11.48-eV resonance. A study of Figs. 3 and 5 shows that many common features may be seen in all three channels. Careful study of data like that shown on Fig. 5(b) indicated that more structure may exist above 12.7 eV, so additional data was obtained at longer dwell time per channel in order to improve the signal to noise ratio. An example of such data is shown in Fig. 6 where four additional structures may be seen. Additional photon data was also obtained at higher-energy resolution, but no additional features were observed.

The gross features observed on both the total and delayed emission functions in the present work are in agreement with those observed previously by Kurzweg, Egbert, and Burns.[10]

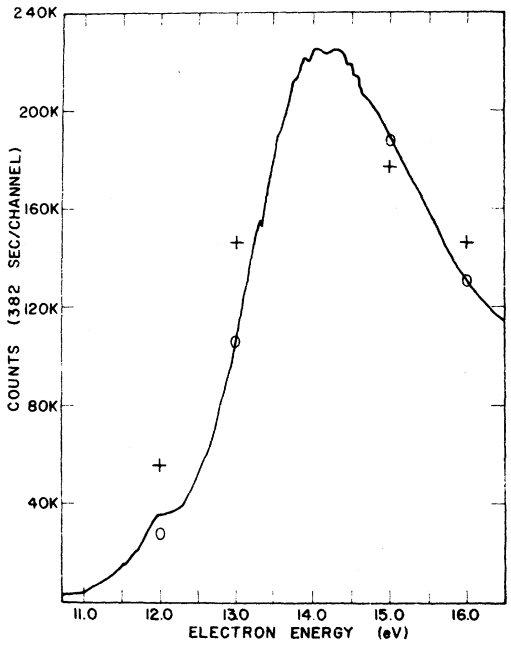

FIG. 4. Total emission function at about 300-meV energy resolution for N_2 $C\,^3\Pi_u \rightarrow B\,^3\Pi_g$ (0, 0) for a range of electron energies from about 11 to 16 eV for 382-sec dwell time per channel and a step size of 16 mV per channel. For comparison, the total emission results of Burns, Simpson, and McConkey (○) (Ref. 17), and the prompt emission results of Kurzweg, Egbert, and Burns (+) (Ref. 10), normalized to the present results at 14 eV, are also shown.

The positions of the features observed in the present work are summarized in Table I, which also includes the previous electron transmission results of Heideman *et al.*[2] and Sanche and Schulz,[6] the differential electron scattering experiments of Comer and Read[3] and Mazeau *et al.*,[7] and the total metastable production experiment of Lawton and Pichanick.[8] The present electron transmission features listed in Table I have been recognized by their repetitive occurrence in a number of sets of data of which Fig. 3 is an example.

As discussed by Schulz,[1] Feshbach resonances are likely to occur below Rydberg-state thresholds in molecules. The lowest Rydberg state of N_2 is $E\,^3\Sigma_g^+$ at 11.87 eV.[24] Thus, the narrow resonance at 11.48 eV first observed by Heideman *et al.*,[2] whose symmetry was designated $^2\Sigma_g^+$ by Comer and Read,[3] is likely to be the Feshbach resonance associated with the lowest $E\,^3\Sigma_g^+$ threshold. The results of Comer and Read[3] have actually shown that a progression of Feshbach resonances associated with the three vibrational thresholds of the $E\,^3\Sigma_g^+$ exists. This series has been designated band "*b*" by Schulz.[1] The first two members of this series are below the lowest E-state threshold, and so are not observed in the delayed $C \rightarrow B$ emission. The first of these (11.48 eV) has been previously observed in the $C \rightarrow B$ emission by Kisker[4] and Finn *et al.*[5] The next feature listed in Table I at 11.87 eV is believed to be a "cusp" on the E-state threshold. This feature appears at 11.87 eV in the electron transmission data of Fig. 3 while no structure at 11.92 eV is observed, also the only feature close in energy in either the delayed-emission function or the total-emission function consistently appears at 11.92 eV. Since this peak appears only in elastic data at 11.87 eV one can conclude that it is an effect due to elastic scattering. Furthermore, a small shoulder can be seen just below the 11.92-eV peak in the delayed emission function [Fig. 5(b) or 6], which could be due to an increase in the elastic scattering cross section near 11.87 eV. This is similar to the feature observed on the $2\,^3S$ threshold in e-He scattering,[25] which has recently been shown in that case to be due to a "cusp" in the elastic scattering cross section at the $2\,^3S$ threshold caused by the opening of a new scattering channel.[26,27] Another feature similar to the one at 11.87 eV has been observed

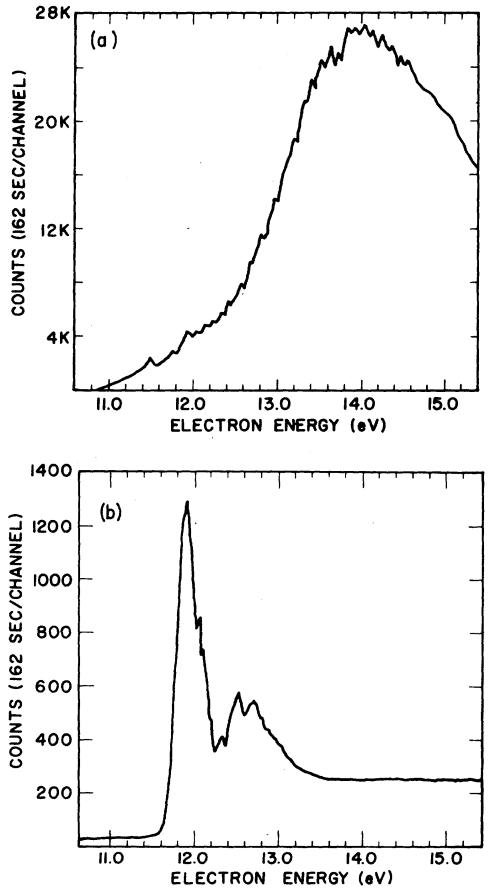

FIG. 5. (a) Total emission function at 100-meV energy resolution for N_2 $C\,^3\Pi_u \rightarrow B\,^3\Pi_g$ (0, 0) for a range of electron energies from 11 to 15.4 eV for 162-sec dwell time per channel and a step size of 16 mV per channel. (b) Delayed emission function at 100-meV energy resolution for N_2 $C\,^3\Pi_u \rightarrow B\,^3\Pi_g$ (0, 0) for a range of electron energies from 11 to 15.4 eV for 162-sec dwell time per channel, a step size of 16 mV per channel, and a delay time of 12 μsec. This emission function is believed to be due to collisional transfer from the $E\,^3\Sigma_g^+$ state as explained in text.

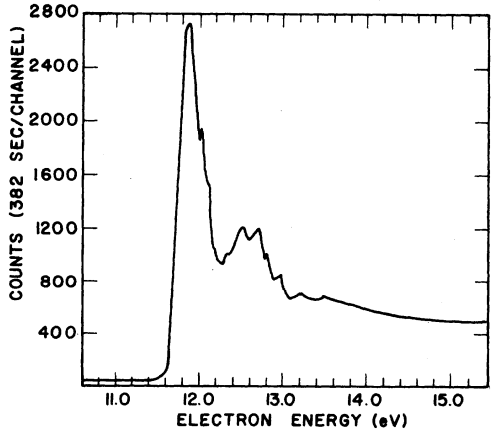

FIG. 6. Delayed emission function at 100-meV energy resolution for N_2 $C\,^3\Pi_u \rightarrow B\,^3\Pi_g$ (0, 0) for a range of electron energies from 11 to 15.4 eV for 382-sec dwell time per channel, a step size of 16 mV per channel, and a delay time of 12 μsec. This emission function is believed to be due to collisional transfer for the $E\,^3\Sigma_g^+$ state, as explained in text.

by Comer and Read at 12.21 eV,[3] and at 12.23 eV by Sanche and Schulz[6] and Lawton and Pichanick.[8] This feature is probably due to the $a''\,^1\Sigma_g^+$ threshold at 12.23 eV. Three additional features are observed between 11.92 and 12.33 eV, which have been identified by Mazeau *et al.*[7] as shape resonances of $^2\Sigma_u^+$ symmetry which they observed to decay to the E and a'' states of N_2. A further three $^2\Pi_u$ shape resonances have been identified by Mazeau *et al.*,[7] through their decay to the E state, which are also observed in the present work with the exception of that near 12.4 eV, which is not recognized in the delayed emission channel. In addition, $^2\Pi_u$ resonances are observed at 12.54 and 12.78 eV which have been observed by Mazeau *et al.*[7] to decay to the E, a'', and C states.[7] Above 12.99 eV, Mazeau *et al.*[7] have identified five members of a $^2\Sigma_u^+$ series of resonances which decay to the E and a'' states of N_2. The first two members of this series are seen in the present delayed emission spectrum while we identify eight members in the present electron transmission and total emission spectra with spacing ~200 meV. The members of this series near the peak in the total emission function [Fig. 5(a)] are seen to contribute strongly to the emission function. At 13.08 eV another series of resonances, also with spacing ~200 meV and which also contributes strongly to the total emission function, appears. This is the first identification of this latter series of reso-

TABLE I. Positions of structures in electron-nitrogen scattering in eV.

	Present			Electron transmission		Differential scattering		
Desig.	Electron transmission (dips)	$C \rightarrow B$ Total emission (peaks)	$C \rightarrow B$ Delayed emission (Peaks)	Elastic only[a]	Elastic and inelastic[b]	Elastic and inelastic[c]	Inelastic[d]	Total metastable production[e]
$^2\Sigma_g^+$	11.48[f]	11.48[f]		11.48	11.49	11.48		
"b"	11.75	11.75		11.75	11.76	11.76		
	12.03	12.02	12.03			12.02		
Threshold	11.87			11.87		11.87		
$^2\Sigma_u^+$		11.92	11.92		11.92		11.90(E,a)	
"shape"	12.15	12.13	12.12				12.15(E,a)	12.15
	12.34	12.34	12.33				12.40(E,a)	
Threshold	12.25	12.23			12.23	12.21		12.23
$^2\Pi_u$							12.14(E)	
"shape"	12.44	12.42					12.40(E)	
	12.68	12.70	12.70		12.64		12.70(E)	
$^2\Pi_u$	12.53	12.55	12.54				12.54(E,a'',C)	12.59
	12.78	12.80	12.80		12.87		12.78(E,a'',C)	12.80
$^2\Sigma_u^+$	12.98	12.98	12.98		13.00		12.99(E,a'',C)	13.03
"$c+d$"	13.21	13.20	13.21		13.23		13.21(E,a'')	13.24
	13.42	13.41					13.45(E,a'')	
	13.63	13.65					13.67(E,a'')	
	13.84	13.84			13.88		13.83(E,a'')	
	14.04	14.05						
	14.24	14.26						
	14.44	14.46						
	13.08							
	13.31	13.33						
	13.52	13.52	13.52		13.50			13.52
	13.74	13.74			13.70		13.72(E,a'')	
	13.94	13.94						
	14.41	14.14			14.12			
	14.34	14.34			14.36			
	14.54	14.54			14.57			

[a] Reference 2.
[b] Reference 6.
[c] Reference 3.
[d] Reference 7.
[e] Reference 8.
[f] Calibration point.

nances, although several members of it have been previously observed.[6,7] (See Table I.) Sanche and Schulz[6] have given the designation "*c*" to resonances whose energies lie between 13.00 and 13.70 eV, and "*d*" to resonances whose energies lie between 13.88 and 14.57 eV. This identification by Sanche and Schulz is in conflict with the subsequent identification of the core excited $^2\Sigma_u^+$ series given by Mazeau *et al.*[7] from differential excitation measurements. Our listing of these two series in Table I follows from the identification of the $^2\Sigma_u^+$ series given by Mazeau *et al.*[7] The second series of resonances (starting out at 13.08 eV) starts out as the weaker of the two, but, probably because of interference effects and due to slight differences in the vibrational constants and the anharmonic terms of the two series, the second series becomes the dominant one at higher energies. It should also be noted that a number of the resonances listed by us, but not listed by Sanche and Schulz,[6] may also be seen in their data.

Finally, it should be stated that the general shape of the delayed photon-emission function is in good agreement with the 0° 11.87-eV energy-loss data of Heideman *et al.*[2] and the total production of metastables experiment of Lawton and Pichanick,[8] with one exception. While the present curve and that of Heideman *et al.*[2] show structure superposed on a background which gradually falls with increasing energy, the curve of Lawton and Pichanick[8] rises with increasing energy. It should be noted that the prompt emission due to direct *C*-state excitation is also rising in this energy domain, and some of the rise in the measured production of metastable may have been due to uv photons.

CONCLUSIONS

This work has demonstrated that the delayed *C*-state emission, which is due to direct population of the *E* state and collisional deactivation to the *C* state, is almost completely due to the decay of many negative-ion states to the *E* state. In addition much of the structure in the peak of the total *C*-state emission function can only be accounted for by decay of the negative-ion states directly to the *C* state. Future work on this transition will study the energy-transfer mechanism between the *E* and *C* states.

ACKNOWLEDGMENT

The authors wish to thank Peter Martin for help with the circuitry.

---

†Work partially supported by the National Science Foundation.

[1]G. J. Schulz, Rev. Mod. Phys. 45, 423 (1973).
[2]H. G. M. Heideman, C. E. Kuyatt, and G. E. Chamberlain, J. Chem. Phys. 44, 355 (1966).
[3]J. Comer and F. H. Read, J. Phys. B 4, 1055 (1971).
[4]E. Kisker, Z. Phys. 257, 51 (1972).
[5]T. G. Finn, J. F. M. Aarts, and J. P. Doering, J. Chem. Phys. 56, 5632 (1972).
[6]L. Sanche and G. J. Schulz, Phys. Rev. A 6, 69 (1972).
[7]J. Mazeau, R. I. Hall, G. Joyex, M. Landau, and J. Reinhardt, J. Phys. B 6, 873 (1973).
[8]S. A. Lawton and F. M. J. Pichanick, Phys. Rev. A 7, 1004 (1973).
[9]R. S. Freund, J. Chem. Phys. 50, 3734 (1969).
[10]L. Kurzweg, G. T. Egbert, and D. J. Burns, Phys. Rev. A 7, 1966 (1973).
[11]D. E. Golden and S. Ormonde, Appl. Phys. Lett. 24, 618 (1974).
[12]D. E. Golden and A. Zecca, Phys. Rev. A 1, 241 (1970).
[13]D. E. Golden and A. Zecca, Rev. Sci. Instrum. 42, 210 (1971).
[14]D. E. Golden, N. G. Koepnick, and L. Fornari, Rev. Sci. Instrum. 43, 1249 (1972).
[15]G. J. Schulz and A. V. Phelps, Rev. Sci. Instrum. 28, 1051 (1957).
[16]The total cross section as given for example by C. Normand, Phys. Rev. 35, 1217 (1930), rises from 10 Å^2 at 12.25 eV to a peak of 11.7 Å^2 at 14.1 eV, while the largest excitation in this energy domain, the direct excitation of the $C\,^3\Pi_u \rightarrow E\,^3\Pi_g$ (0, 0), as given for example by Ref. 10, varies from 0.0149 Å^2 at 12 eV to 0.118 Å^2 at 14 eV. The data of Ref. 10 has been normalized to that of Ref. 17. at 14 eV.
[17]D. J. Burns, F. R. Simpson, and J. W. McConkey, J. Phys. B 2, 52 (1969).
[18]J. D. Jobe, F. A. Sharpton, and R. M. St. John, J. Opt. Soc. Am. 57, 106 (1967).
[19]J. F. M. Aarts, F. J. DeHeer, Chem. Phys. Lett. 4, 116 (1969).
[20]S. Ormonde and D. E. Golden, Phys. Rev. Lett. 31, 1161 (1973).
[21]See also, G. Gould, Appl. Opt. Suppl. 2, 59 (1965).
[22]R. S. Stolarski, V. A. L. Dulock, C. E. Watson, and A. E. S. Green, J. Geophys. Res. 72, 3953 (1967).
[23]D. C. Cartwright, Phys. Rev. A 2, 1331 (1970).
[24]R. S. Mulliken, in *The Threshold of Space*, edited by M. Zelikoff (Pergamon, New York, 1957).
[25]L. Sanche and G. J. Schulz, Phys. Rev. A 5, 1672 (1972).
[26]S. Cvejanovic, J. Comer, and F. H. Read, J. Phys. B 7, 468 (1974).
[27]D. E. Golden, F. D. Schowengerdt, and J. Macek, J. Phys. B 7, 478 (1974).